Differential Molecular and Cellular Immune Mechanisms of Postoperative and Lps-Induced Ileus in Mice and Rats

Joachim Schmidt[*,1,3], **Burkhard Stoffels**[*,1,4], **R. Savanh Chanthaphavong**[2], **Bettina M. Buchholz**[1,4], **Atsunori Nakao**[2], and **Anthony J. Bauer**[1]

[1]Department of Medicine/Gastroenterology, University of Pittsburgh, Pittsburgh, PA

[2]Department of Surgery, University of Pittsburgh, Pittsburgh, PA,

[3]Department of Surgery, University of Münster, Münster, Germany

[4]Department of Surgery, University of Bonn, Bonn, Germany

Abstract

Ileus is caused by the initiation of a complex cascade of molecular and cellular inflammatory responses within the intestinal muscularis, which might be species specific. Our objective was to investigate a possible immunological divergence in the mechanisms of postoperative- and endotoxin-induced ileus in C57BL/6 mice and Sprague-Dawley rats.

Gastrointestinal transit (GIT) was measured at 24 hour after the injurious stimulus. MPO-staining and F4/80 immunohistochemistry were used to quantify polymorphonuclear and monocyte infiltration of jejunal muscularis whole-mounts, and intestinal muscularis MCP-1, ICAM-1 and iNOS gene expression was assessed by RT-PCR. Intestinal muscularis subjected to *in vivo* surgical manipulation (SM) or LPS treatment was cultured for 24 hours, and the liberation of nitric oxide and chemokines/cytokines into the culture medium was analyzed by Griess reaction and Luminex multiplex assay.

Intestinal SM and lipopolysaccharide (LPS) (15mg/kg) caused a significant delay in gastrointestinal transit, which was more severe in mice compared to rats in both injury models. Both SM- and LPS-triggered neutrophil and monocytic extravasation into the rat jejunal muscularis exceeded the cellular infiltration seen in mice. These results correlated with significantly greater increases in rat muscularis MCP-1 (syn. CCL2), ICAM-1 and iNOS message with more subsequent NO production after SM or LPS compared to mouse. The cultured muscularis obtained from SM mice released significantly more inflammatory proteins such as TNF-α, IL-1-α, IL-4 and GM-CSF compared to the manipulated rat muscularis. In contrast, LPS initiated the secretion of significantly more IL-1β by the inflamed rat muscularis compared to the mouse, but GM-CSF (syn. CSF2) liberation from mouse muscularis was markedly higher compared to LPS-treated rat muscularis.

The data indicate that mechanistically the development of ileus in rat is mediated predominately through a leukocytic pathway consisting of chemotaxis, cellular extravasation and NO liberation.

Correspondence/Reprints: Anthony J. Bauer, Ph.D. Department of Medicine/Gastroenterology University of Pittsburgh S-849 Scaife Hall, 3550 Terrace Street Pittsburgh, Pennsylvania 15261 tbauer@pitt.edu Phone: (412) 648-7204 Fax: (412) 648-9731.
*both authors contributed equally

Whereas, the more intense mouse ileus evolves via a potent but injury-specific local cytokine response.

Keywords

ileus; inflammation; endotoxin; sepsis; surgery; postoperative ileus

---

1. Introduction

In many respects the small intestine remains a virtual "black box", especially when it comes to understanding clinical motility disorders. Postoperative ileus (POI), the postsurgical impairment of propulsive gastrointestinal motility [1-4], frequently occurs after major abdominal surgical procedures [5;6], and also following extra-abdominal operations [7;8]. Sepsis and multiple-organ failure, which account for the leading causes of morbidity and mortality in the critically ill [9-11], can develop in the sequela of non-resolving POI. Reciprocally, sepsis often times triggers ileus.

In the recent past, we and others have shown that the intestinal muscularis externa itself actively participates in the immunological pathogenesis of postoperative and endotoxin-induced ileus [6;12;13]. Furthermore, it is now appreciated that the gastrointestinal muscularis is populated with an extraordinarily dense network of macrophages [10;14;15]. Importantly, simple intraoperative intestinal handling of the bowel or endotoxin exposure results in the activation of these resident macrophages, which leads to the activation of transcription factors (NF-κB, NF-IL-6, STAT-3 and Egr-1) as well as the induction and liberation of various cytokines/chemokines such as IL-6, TNF-α, IL-1β and MCP-1 and immune stimulant factors like VEGF and GM-CSF. Subsequently, vascular adhesion molecules (ICAM-1 and LFA-1) are upregulated, leukocytes are recruited into the intestinal muscularis externa and leukocyte-derived motility inhibiting mediators such as nitric oxide and prostaglandin E2 are released via inducible nitric oxide synthase and cyclo-oxygenase-2 [13;16].

To fully investigate the complex molecular and cellular immune phenomena in ileus, scientists oftentimes rely on animal models for which rodents like mice and rats are commonly employed. The appropriate extrapolation of these data to the clinical field requires an integrated understanding of the relative importance of the individual mechanisms along with the consideration of a possible species differences in these mechanisms.

To our knowledge, there has been no direct study systematically comparing the mechanisms of ileus in mouse and rat. We, therefore, designed a comparative study specifically investigating similarities and differences in the inflammatory mechanisms of ileus between mice and rats. Concomitantly, we also sought to elucidate common inflammatory signaling pathways within the models of postoperative ileus and endotoxemia.

2. Materials and Methods

2.1. Animals and experimental groups

Male C57BL/6 mice weighing 20-25g and male Sprague Dawley rats weighing 300-350g (Harlan, Indianapolis, Indiana) were housed in a pathogen-free facility that is accredited by the American Association for Accreditation of Laboratory Animal Care and which complies with the requirements of humane animal care as stipulated by the United States Department of Agriculture and the Department of Health and Human Services. The research protocol was approved by the Institutional Animal Use and Care Committee of the University of

Pittsburgh. Animals were maintained on a 12-hour light/dark cycle and provided with commercially available chow and tap water *ad libitum*. Animals of both species were randomly subjected either to control, sham saline injection, surgical manipulation (SM) of the small bowel or intraperitoneal LPS injection (N=5 each group and each experiment). Control and sham saline injection yielded similar results in all experiments performed. Therefore, the data of these groups were pooled and are referred to as control group.

2.2. Animal Model of POI

Ileus was induced in mice and rats by a standardized gut manipulation procedure, as described by Kalff et al. [6]. In brief, a midline laparotomy was carried conditions out during isoflurane anesthesia. The small intestine was carefully eventrated under sterile and gently compressed from the ligament of Treitz to the terminal ileum using a rolling motion of two moist cotton-tipped applicators. To ensure similar manipulation of all intestinal segments, this running procedure was repeated three times. The intestine was then returned to the peritoneal cavity and the incision was closed in a two layer fashion with running 4-0 silk sutures.

2.3. Animal Model of Sepsis

Mice and rats underwent a light isoflurane anesthesia and received an intraperitoneal LPS (Sigma-Aldrich Co, St. Louis, MO, USA) injection at the dose of 15mg/kg LPS. Age-matched sham-treated mice and rats were injected with equal volumes of saline.

2.4. Determination of gastrointestinal transit

To determine the effects of intestinal manipulation and endotoxin-induced sepsis on gut motility, we measured the aboral transit of a non-absorbable tracer, fluorescein isothiocyanate-labeled dextran with an average molecular mass of 70 kDa (FD70), as previously described [17;18]. Briefly, mice were fed with 10 μl and rats with 20 μl of FD70 dissolved in distilled water (6.25 mg/ml) by gavage. Ninety minutes later, the entire gastrointestinal tract, from the lower esophageal sphincter to the descending colon, was excised and divided into 15 segments: stomach, small intestine (10 segments of equal length), cecum, and colon (three segments of equal length). Supernatants of the intestinal chyme were fluorometrically assayed for the FD70 concentration. The gastrointestinal distribution of FD70 was analyzed by calculating the geometric center (GC) using the following formula; GC= (% of total fluorescent signal per segment x segment number)/ 100 [19].

2.5. Measurement of nitric oxide in muscularis cultured supernatant

In all groups, the harvested small intestine was transferred to a sterile beaker containing DMEM culture medium supplemented with 200 U/ml penicillin G and 200 μg/ml streptomycin. The muscularis externa was isolated from the mucosa/lamina propria, and aliquots of 70–100 mg were cultured in supplemented DMEM in a CO2-controlled incubator (NuAire, Plymouth, MN). After an incubation period of 24 hours, the supernatant was frozen in liquid nitrogen and stored at −80°C. The muscle tissue was blotted dry and weighed. The concentration of nitrite, a stable metabolite of nitric oxide (NO), in the culture media was assayed by a standard Griess reaction, as described previously [20]. Griess reagent was prepared by mixing equal volumes of sulfanilamide (1.5% in 5% H3PO4) and naphthylethylenediamine dihydrochloride (0.1% in H2O). A volume of 100 μl of reagent was mixed with 100 μl of supernatant and incubated at room temperature for 10 min. Absorbance of the formed chromophore was measured at 540 nm in an automated microplate reader. Nitrite was quantified using serial dilutions of NaNO2 as a standard and results were expressed as μM/g nitrite.

2.6. Luminex Multiplex Bead Immunoassays

The release of multiple inflammatory analytes into the tissue culture supernatant, obtained as above, was quantified with a Luminex 100™ using microsphere-based multiplexing technology (Invitrogen Corporation, Carlsbad, CA). The mouse Twenty-Plex immune kit was comprised of analyte specific components for the simultaneous measurement of the mouse cytokines: FGF basic, GM-CSF, IFN-γ, IL-1α, IL-1β, IL-2, IL-4, IL-5, IL-6, IL-10, IL-12p40/p70, IL-13, IL-17, IP-10, KC, MCP-1, MIG, MIP-1α and TNF-α. The rat Ten-Plex immune kit comprised of analyte specific components for the simultaneous measurement of rat cytokines: GM-CSF, IFN-γ, IL-1β, IL-2, IL-4, IL-5, IL-6, IL-10, IL-12 and TNF-α.

2.7. Histo- and immunohistochemistry stainings

Mid-jejunal segments, either fixed in 100% ethanol or 4% paraformaldehyde, were microdissected (Leica MZ9-5, W. Nuhsbaum, Inc., McHenry, IL) and ½ x 1cm measuring mucosa-free muscularis whole-mounts were used for myeloperoxidase staining procedures [21]. Recruited polymorphonuclear neutrophils (PMN) were visualized by a stain through immersing in a mixture of 10mg Hanker-Yates reagent (Sigma, St. Louis, MO), 10mL KRB and 10μL 3% hydrogen peroxide for 20 minutes. For immunohistochemical quantification of infiltrating monocytes, muscularis whole-mounts were incubated with rat polyclonal anti-mouse F 4/80 antibody conjugated to ALEXA 488 (1:200, Serotec, cross-reacting with rat) for 24 hours at 4°C. All specimens were inspected by light or fluorescent microscopy after staining (Leica DMRX, W. Nuhsbaum, Inc., McHenry, IL). Immunocytes were counted in 5 randomly chosen areas in each specimen at a magnification of 200x.

2.8. RNA extraction and mRNA expression

Isolated intestinal muscularis of mice and rats was harvested at a series of specific time points after intestinal manipulation and endotoxin induced sepsis (0, 1.5, 6 and 24 hours) and stored at −80 °C until analysis. Total RNA extraction was performed using the guanidinium thiocyanate phenol-chloroform extraction method [12]. iNOS, ICAM-1 and MCP-1 mRNA expression was quantified in duplicate by SYBR Green two-step, real-time RT-PCR (ABI PRISM 7700 Sequence Detection System, PE Applied Biosystems). Primers were designed according to published sequences and GenBank accession numbers using Primer Express software (PE Applied Biosystems, Foster City, CA). The sequences of the real-time-PCR primers for both species are listed in Tables 1 and 2. Real-time PCR data were plotted as the ΔRn fluorescence signal versus the cycle number to determine the threshold cycle (CT). Target-specific mRNA expression was normalized to the endogenous GAPDH housekeeping gene and calculated relative to control using the comparative CT method.

2.9. Solutions and Statistics

A standard Krebs Ringers buffer (KRB) was used as described previously. This physiologic solution was gassed with 97% O_2, 3% CO_2 to establish a pH of 7.4. KRB constituents were obtained from Sigma Chemical Company (St. Louis, MO). Results are presented as means ± standard error of the mean (SEM). EZAnalyze ANOVA was used to perform the F-test and Bonferroni post-hoc group comparisons where appropriate. P values < 0.05 were considered significant.

3. Results

3.1. Effects of surgical manipulation and endotoxin-induced sepsis on intestinal muscle function

In vivo gastrointestinal transit (GIT) was performed to evaluate potential functional differences between the species in the models of intestinal manipulation and endotoxemia. As shown in the distribution histogram in Figure 1A, the fluorescently labeled dextran was transported aborally in both mouse and rat control groups with the peak signal detected in the terminal ileum. As predicted from previous observations, surgical manipulation of the intestine of mice and rats caused a significant delay in gastrointestinal transit with the maximal fluorescence accumulating in the duodenum and proximal jejunum. Interestingly, the calculated postoperative delay in gastrointestinal transit was significantly greater in mice compared to rats, even though a similar manipulation procedure was performed in both species ($p < 0.05$, N=5) (Figure 1C).

Lipopolysaccharide (LPS) injection is known to cause a dose dependent decrease in gastrointestinal transit time [10;12]. An LPS dose of 15mg/kg was chosen in this study because it inflicts a relatively similar delay in gastrointestinal transit as the standard surgical manipulation procedure does in mice. Figure 1B shows the averaged transit distribution patterns in both endotoxin injected species compared to their respective control. Again, as seen after surgical manipulation, the LPS injected mice showed a significantly more delayed transit time compared to the LPS injected rats as demonstrated by the calculated geometric center ($p < 0.05$, N=5) (Figure 1C).

3.2. Intestinal muscularis neutrophil infiltration

Previously, we have shown a correlation between the post-surgical and endotoxin-induced suppression in circular smooth muscle function and leukocyte infiltration into the intestinal muscularis[10;22]. Therefore, we sought to quantify the recruitment of neutrophils into the muscularis externa of both species to correlate it with the above obtained species-specific functional results. As we have demonstrated in the past, control whole-mounts contained only an occasional neutrophil, and surgical manipulation resulted in the recruitment of a large number of neutrophils into the muscularis externa of both species. LPS injection into both species also recruited a significant number of neutrophils into the muscularis compared to controls as shown in the histogram in Figure 2A. However, statistical analysis of the mean data showed that in both models there was a significantly higher recruitment of neutrophils in rats compared to mice ($p < 0.05$), even though gastrointestinal transit was impaired to a greater degree in mice.

3.3. Intestinal muscularis monocyte infiltration

A correlation between the development of inflammatory ileus and a monocytic infiltration into the intestinal muscularis after surgical trauma and endotoxin-induced sepsis has been made in rats [10;23]. After revealing a greater extravasation of neutrophils into the rat intestinal muscle layer compared to mice, we speculated that the functional impairment in mice could be attributable to a higher recruitment of monocytes. Figure 2B shows representative pictures from whole-mounts from controls and 24 hours after SM or LPS injection of mouse and rat. Control whole-mounts contained only few F4/80 positive monocytes in both species, and surgical manipulation of the intestine or LPS injection resulted in the recruitment of a significant number of monocytes into the intestinal muscularis. The histogram in Figure 2C shows the quantification of F4/80 positive monocytes in whole-mounts from the six groups of animals in our study. Statistical analysis of the mean data not only showed the previously described significant difference between the number of monocytes in control whole-mounts versus whole mounts from SM or LPS injected animals

of both species, but also a major difference in the degree of infiltration between both rodent species (t-test, p<0.05, N=5). Unlike from what could have been expected from the functional transit data, but similar to the analysis of neutrophil infiltration, the rat muscularis whole mounts displayed a 3-fold higher number of F4/80 positive cells in the SM model and a 2-fold higher count of extravasated monocytes in the LPS injected groups compared to the C57BL/6 mice.

3.4. Proinflammatory mRNA induction time profiles

To investigate a cause for the observed difference in the degree of muscularis leukocytic infiltration between both species occurring in response to both inflammatory insults, we sought to determine the mRNA induction of chemokine monocyte chemoattractant protein-1 (MCP-1, syn. CCL2) and intercellular adhesion molecule-1 (ICAM-1). Both molecules have previously been shown to promote monocyte and leukocyte infiltration into the jejunal muscle layer, respectively [24;25]. In rat, surgical manipulation and LPS rapidly and markedly induced MCP-1 mRNA within the muscularis externa (Figure 3A and 3B). MCP-1 mRNA induction peaked 90 minutes after surgery with a 156-fold induction over control and remained significantly elevated for up to 24 hours. This induction pattern in rat was relatively similar for LPS. Although, MCP-1 mRNA was significantly induced in the mouse by both surgical manipulation and LPS, the levels were markedly lower compared to rat at similar time points. After surgical manipulation of the mouse, MCP-1 mRNA reached its peak induction of only 8-fold after 6 hours and returned back to control levels by 24 hours. In LPS injected mice, we observed an early 15-fold upregulation in muscularis MCP-1 mRNA, which persisted throughout the 24 hour period of analysis.

MCP-1 induces endothelial ICAM-1, and ICAM-1 plays a direct role in leukocyte recruitment. Investigating ICAM-1 mRNA yielded analogous results to MCP-1 (Figure 3C and 3D). The inflamed surgically manipulated rat muscularis showed a rapid induction of ICAM-1 mRNA reaching its peak at 90 min (23-fold) and remained elevated to 24 hours. The LPS injected rat also followed this pattern, reaching the highest point of induction at 90 minutes (78-fold), which was followed by a gradual down regulation over the 24 hour period of analysis. Parallel to mouse MCP-1 expression levels, ICAM-1 levels were also significantly induced with a similar temporal mechanistically profile but again to a lesser degree than in the rat (p<0.05) (Figure 3C and 3D). This could explain the greater number of recruited neutrophils and monocytes into the rat muscularis after surgery or LPS compared to the mouse.

3.4. Muscularis iNOS mRNA and NO release

Previously, the induction of iNOS and the production of NO, has been shown to play a critical role as a kinetically active smooth muscle inhibitor mediating ileus following surgery and endotoxin injection [12;26]. Similar to previous studies, we detected a significant upregulation in iNOS mRNA expression following surgical manipulation within the rat muscularis externa at 90 minutes and 6 hours up to 33-fold (Figure 4A). In the rat LPS-induced sepsis model, we observed a 3-fold induction of iNOS within the rat muscle layer at 90 minutes with a peak at 6 hours. Twenty-four hours following injection, the expression of iNOS waned back to near its respective control level. For the C57BL/6 mice, we detected a constant 2-fold to 4-fold iNOS upregulation after surgical manipulation over the time period of 24 hours. Analogous observations with iNOS gene induction of 3-fold to 8-fold of baseline levels were made in the C57Bl6 mouse after LPS injection (Figure 4B).

Hence, once again we saw a significantly higher induction of this inhibitor of smooth muscle contraction in the rat compared to the mouse. Ninety minutes after surgical trauma, the induction of iNOS was 17-fold higher and at 6 hours it was 8-fold higher in the rat compared

to the mouse (p<0.05). In parallel, we saw a significantly higher induction in the rat muscularis in the endotoxin sepsis model (4-fold at 6 hours compared to mouse) (p<0.05). Comparable to the observed dissimilar induction levels of iNOS mRNA, we were able to reveal a significant difference in the extent of NO released from the organ cultured muscularis externa between the two species in both inflammatory models (Figure 4C and 4D). The surgical trauma resulted in a 2-fold higher release of NO in the rats compared to the mice, while in the endotoxin-sepsis model the inflamed rat muscularis released 4-fold more nitric oxide compared to the mouse (p<0.05, N=5 each).

3.5. Inflammatory mediators released by the cultured intestinal muscularis

Analysis of intestinal muscularis-derived inflammatory proteins is hypothesized to suggest the existence of immunological mechanisms in the pathogenesis of ileus in both injury models. The release of ten cytokines (TNF-α, IL-1α, IL-1β, IL-2, IL-4, IL-6, IL-10, IL-12p40/p70, GM-CSF and IFN-γ) by the cultured muscularis was analyzed in both species. In contrast to inflammatory mediators reported above, the postoperative mouse muscularis externa released quantitatively more TNF-α, IL-1α, IL-4 and GM-CSF compared to the rat muscularis externa (Figure 5A-F) (p<0.05). And, following LPS injection, the mouse muscularis externa released quantitatively more GM-CSF compared to the rat (p<0.05), whereas, IL-6, IL-10, IL-12 and IFN-γ protein levels secreted by the muscularis after surgery and LPS were similar between mouse and rat (Figure 5E **for IL-6 and data not shown**) (p>0.05). By contrast, measured IL-1β levels were higher in rat compared to mouse in both models (p<0.05).

4. Discussion

A wide range of scientific investigations aiming to ultimately elucidate the pathophysiology of human disease is primarily done in animals. However, all animal models have shortcomings which need to be considered, since they do not exactly duplicate the human illness. Therefore, a comprehensive understanding of species diversity is crucial to the general comprehension of disease mechanisms. In fact, even distinct mouse strain differences have been demonstrated when they are exposed to LPS from the same vendor using an identical dose [27]. Yet, considerable immunological and therapeutic evidence suggests that immune-mediated models are relevant to human diseases and that many pathogenic principles are similar. In particular, postoperative inflammatory molecular data demonstrated that an iatrogenic-induced molecular inflammatory response within the muscularis externa does occur during human surgery and a pilot study demonstrating the importance of mast cells are all common features also observed in mice and rats [28-30].

Therefore, the objective of this study was to comparatively investigate the mechanisms of postoperative and endotoxin-induced ileus and, at the same time, to reveal similarities and differences in the inflammatory mechanisms from the most widely used rodents, namely rat and mouse. Our work clearly shows that the molecular, cellular and functional pathophysiology of these distinctly different models have unique characteristics because a relatively different constellation of inflammatory events orchestrate the development of ileus in each species and in each model. Hence, caution is needed when assessing the mechanistic aspects of diseased animal models in various species.

Specifically, the results demonstrate that the mouse exhibits a more severe delay in gastrointestinal transit in response to surgical manipulation and endotoxin compared to the rat. Interestingly, however, the rat develops a significantly greater leukocytic inflammatory response which correlates with a species specific exuberant induction of mRNAs for chemo-attractant MCP-1 (syn. CCL2) and ICAM-1. Furthermore, the rat displayed a greater induction of intestinal muscularis iNOS mRNA and a subsequent greater release of NO from

the organ cultured muscularis externa. However, in contrast, the mouse muscularis externa released quantitatively more TNF-α, IL- α, IL-4 and GM-CSF (syn. CSF2) compared to the rat muscularis externa. Furthermore, the postoperative ileus model produced a greater molecular and cellular inflammatory response compared to endotoxemia.

The species differences in gastrointestinal motility to LPS *in vivo* were apparently not due to an increased sensitivity of the contractile motor unit (smooth muscle/ICC) of the mouse, because the LPS dose response suppression of jejunal circular muscle contractile activity *in vitro* is relatively similar between these two species[10;12;31]. In an effort to reveal species and model specific mechanisms of ileus, the relatively large LPS dose of 15mg/kg was chosen in this study, particularly because it inflicts a relatively similar delay in gastrointestinal transit as the standard surgical manipulation procedure in each species. As in the POI model, the mouse had quantitatively fewer leukocytic cellular infiltrates compared to the rat for both neutrophils and monocytes. Mechanistically, this species difference could be attributed to the higher and more sustained mRNA levels of MCP-1, because MCP-1 is known to potently cause leukocyte recruitment through an induction of ICAM-1, which indeed was also more significantly expressed in both rat models compared to the mouse. Blockade of MCP-1 and ICAM-1 was shown to ameliorate the inflammatory response and ileus in rats giving evidence of the causative role of recruited and activated leukocytes in ileus[24;25]. Interestingly, although both injury models produced a similar degree of paralytic ileus, the relative degree of leukocytic cellular infiltrates was strikingly greater in the POI model compared to endotoxemia in both species. These data indicate that the contribution of the recruited neutrophils and monocytes and the subsequently released inflammatory mediators into the interstitial milieu of the muscularis externa is markedly species and injury specific in causing ileus. And, we may add that these responses are most likely age-dependent, as we have shown previously in the postoperative ileus model[13].

One of the proposed important mediators of ileus is the enteric induction of iNOS (synonymous NOS2) and the sustained tonic leukocyte-derived release of nitric oxide into the muscularis interstitium[12;26;32]. Previously, using iNOS$^{-/-}$ mice and pharmacological inhibition, the role of active nitric oxide production from both the postoperative rat and mouse muscularis was clearly demonstrated[16;26]. Interestingly, in the rat POI model the peak induction of iNOS mRNA occurs relatively early at 90 min which transpired before leukocyte recruitment takes place. Hence, we assume that the resident network of macrophages accounts for the muscularis cellular population that primarily contributed to this early elevated expression. Currently, it remains to be determined whether NO contributes to ileus primarily via its direct suppressive effect on smooth muscle or by its role as a gaseous signaling molecule. Interestingly, however, rats had relatively a more resilient gastrointestinal transit to insult compared to the mouse which importantly had a comparatively diminished activation of this molecular inflammatory cascade indicating the existence of additional mechanisms of ileus in the mouse.

In contrast to the rather leukocyte dominated inflammatory response in both rat models of ileus, the mouse muscularis inflammatory milieu demonstrated a greater molecular inflammatory cytokine response which consisted of TNF-α, IL-1 α, IL-4 and GM-CSF/ CSF2 liberation. In particular, GM-CSF was secreted markedly more in both mouse models. However, secreted IL-6, IL-10, IL-12 and IFN-γ protein levels showed no interspecies variability within the individual models of either postoperative ileus or endotoxemia. In contrast, IL-1β protein secretion by the muscularis was singularly higher in rat compared to mouse in both models. The direct functional significance of the muscularis inflammatory milieu has been studied by the laboratories of Moody and Collins. Specifically, Lodato et. al. presented evidence in the rat endotoxin model that combined *in vivo* pretreatment with TNF-α binding protein and an IL-1 receptor antagonist significantly blunted the LPS

induction of iNOS, which subsequently improved *in vitro* muscle contractility[33]. Additionally, it has been shown that IL-1β suppresses norepinephrine release from the myenteric plexus and that combined IL-1β and IL-6 synergistically diminish enteric neurotransmitter release[34].

In conclusion, these data demonstrate that a relatively different constellation of inflammatory events orchestrate the development of ileus in each species. Furthermore, the results provide insight into the quest of elucidating the critical inflammatory mechanisms of ileus in the clinically important syndromes of postoperative and sepsis induced ileus.

Acknowledgments

Abbreviations

C_T	cycle threshold
COX-2	cyclooxygenase-2
GAPDH	glyceraldehyde phosphate dehydrogenase
GC	geometric center
ICAM-1	intercellular adhesion molecule-1
IL-6	interleukin-6
iNOS	inducible nitric oxide synthase
KRB	Krebs-Ringer buffer
LPS	lipopolysaccharide
MCP-1	monocyte chemoattractant protein-1
MPO	myeloperoxidase
NO	nitric oxide
PBS	phosphate-buffered saline
PGE	prostaglandin
PMN	polymorphonuclear neutrophils
RT-PCR	reverse transcriptase polymerase chain reaction
SM	surgical manipulation

Reference List

(1). Holte K, Kehlet H. Postoperative ileus: a preventable event. Br J Surg. 2000; 87:1480–1493. [PubMed: 11091234]

(2). Livingston EH, Passaro EP Jr. Postoperative ileus. DDS. 1990; 35:121–132.

(3). Bauer AJ, Boeckxstaens GE. Mechanisms of postoperative ileus. Neurogastroenterol Motil. 2004; 16(Suppl 2):54–60. [PubMed: 15357852]

(4). Kehlet H. Postoperative ileus. Gut. 2000; 47(Suppl 4):iv85–iv86. [PubMed: 11076929]

(5). Luckey A, Livingston E, Tache Y. Mechanisms and treatment of postoperative ileus. Arch Surg. 2003; 138:206–214. [PubMed: 12578422]

(6). Kalff JC, Schraut WH, Simmons RL, Bauer AJ. Surgical manipulation of the gut elicits an intestinal muscularis inflammatory response resulting in postsurgical ileus. Ann Surg. 1998; 228:652–663. [PubMed: 9833803]

(7). Bederman SS, Betsy M, Winiarsky R, Seldes RM, Sharrock NE, Sculco TP. Postoperative ileus in the lower extremity arthroplasty patient. J Arthroplasty. 2001; 16:1066–1070. [PubMed: 11740765]

(8). Gonzalez OA, Orozco MA, Barrera ZL, et al. Abdominal complications after cardiopulmonary procedures. Rev Gastroenterol Mex. 1999; 64:61–69. [PubMed: 10532129]

(9). Cumming J, Purdue GF, Hunt JL, O'Keefe GE. Objective estimates of the incidence and consequences of multiple organ dysfunction and sepsis after burn trauma. J Trauma. 2001; 50:510–515. [PubMed: 11265031]

(10). Eskandari MK, Kalff JC, Billiar TR, Lee KK, Bauer AJ. Lipopolysaccharide activates the muscularis macrophage network and suppresses circular smooth muscle activity. Am J Physiol. 1997; 273:G727–G734. [PubMed: 9316478]

(11). Jiang J, Bahrami S, Leichtfried G, Redl H, Ohlinger W, Schlag G. Kinetics of endotoxin and tumor necrosis factor appearance in portal and systemic circulation after hemorrhagic shock in rats. Ann Surg. 1995; 221:100–106. [PubMed: 7826148]

(12). Eskandari MK, Kalff JC, Billiar TR, Lee KK, Bauer AJ. LPS-induced muscularis macrophage nitric oxide suppresses rat jejunal circular muscle activity. Am J Physiol. 1999; 277:G478–G486. [PubMed: 10444463]

(13). Bauer AJ. Mentation on the immunological modulation of gastrointestinal motility. Neurogastroenterol Motil. 2008; 20(Suppl 1):81–90. [PubMed: 18402645]

(14). Mikkelsen HB. Macrophages in the external muscle layers of mammalian intestines. Histol Histopathol. 1995; 10:719–736. [PubMed: 7579823]

(15). Kalff JC, Schwarz NT, Walgenbach KJ, Schraut WH, Bauer AJ. Leukocytes of the intestinal muscularis: their phenotype and isolation. J Leukoc Biol. 1998; 63:683–691. [PubMed: 9620660]

(16). Turler A, Kalff JC, Moore BA, et al. Leukocyte-derived inducible nitric oxide synthase mediates murine postoperative ileus. Ann Surg. 2006; 244:220–229. [PubMed: 16858184]

(17). Moore BA, Otterbein LE, Turler A, Choi AM, Bauer AJ. Inhaled carbon monoxide suppresses the development of postoperative ileus in the murine small intestine. GE. 2003; 124:377–391.

(18). Moore BA, Turler A, Pezzone MA, Dyer K, Grandis J, Bauer AJ. Tyrphostin AG 126 inhibits development of postoperative ileus induced by surgical manipulation of murine colon. Am J Physiol Gastrointest Liver Physiol. 2004; 286:G214–G224. [PubMed: 14512290]

(19). Miller MS, Galligan JJ, Burks TF. Accurate measurement of intestinal transit in the rat. J Pharmacol Methods. 1981; 6:211–217. [PubMed: 7329070]

(20). Xiong H, Zhu C, Li F, et al. Inhibition of interleukin-12 p40 transcription and NF-kappaB activation by nitric oxide in murine macrophages and dendritic cells. J Biol Chem. 2004; 279:10776–10783. [PubMed: 14679201]

(21). Moore BA, Overhaus M, Whitcomb J, et al. Brief inhalation of low-dose carbon monoxide protects rodents and swine from postoperative ileus. Crit Care Med. 2005; 33:1317–1326. [PubMed: 15942350]

(22). Kalff JC, Carlos TM, Schraut WH, Billiar TR, Simmons RL, Bauer AJ. Surgically induced leukocytic infiltrates within the rat intestinal muscularis mediate postoperative ileus. GE. 1999; 117:378–387.

(23). Kalff JC, Buchholz BM, Eskandari MK, et al. Biphasic response to gut manipulation and temporal correlation of cellular infiltrates and muscle dysfunction in rat. Surgery. 1999; 126:498–509. [PubMed: 10486602]

(24). Kalff JC, Hierholzer C, Tsukada K, Billiar TR, Bauer AJ. Hemorrhagic shock results in intestinal muscularis intercellular adhesion molecule (ICAM-1) expression, neutrophil infiltration, and smooth muscle dysfunction. Arch Orthop Trauma Surg. 1999; 119:89–93. [PubMed: 10076954]

(25). Turler A, Schwarz NT, Turler E, Kalff JC, Bauer AJ. MCP-1 causes leukocyte recruitment and subsequently endotoxemic ileus in rat. Am J Physiol Gastrointest Liver Physiol. 2002; 282:G145–G155. [PubMed: 11751168]

(26). Kalff JC, Schraut WH, Billiar TR, Simmons RL, Bauer AJ. Role of inducible nitric oxide synthase in postoperative intestinal smooth muscle dysfunction in rodents. GE. 2000; 118:316–327.

(27). Yang IV, Wade CM, Kang HM, et al. Identification of novel genes that mediate innate immunity using inbred mice. Genetics. 2009; 183:1535–1544. [PubMed: 19805818]

(28). Engel DR, Koscielny A, Wehner S, et al. T helper type 1 memory cells disseminate postoperative ileus over the entire intestinal tract. Nat Med. 2010; 16:1407–1413. [PubMed: 21113155]

(29). Kalff JC, Turler A, Schwarz NT, et al. Intra-abdominal activation of a local inflammatory response within the human muscularis externa during laparotomy. Ann Surg. 2003; 237:301–315. [PubMed: 12616113]

(30). The FO, Buist MR, Lei A, et al. The role of mast cell stabilization in treatment of postoperative ileus: a pilot study. Am J Gastroenterol. 2009; 104:2257–2266. [PubMed: 19491822]

(31). Buchholz BM, Chanthaphavong RS, Bauer AJ. Nonhemopoietic cell TLR4 signaling is critical in causing early lipopolysaccharide-induced ileus. J Immunol. 2009; 183:6744–6753. [PubMed: 19846874]

(32). Cullen JJ, Mercer D, Hinkhouse M, Ephgrave KS, Conklin JL. Effects of endotoxin on regulation of intestinal smooth muscle nitric oxide synthase and intestinal transit. Surgery. 1999; 125:339–344. [PubMed: 10076620]

(33). Lodato RF, Khan AR, Zembowicz MJ, et al. Roles of IL-1 and TNF in the decreased ileal muscle contractility induced by lipopolysaccharide. Am J Physiol. 1999; 276:G1356–G1362. [PubMed: 10362638]

(34). Ruhl A, Hurst S, Collins SM. Synergism between interleukins 1 beta and 6 on noradrenergic nerves in rat myenteric plexus. Gastroenterology. 1994; 107:993–1001. [PubMed: 7926489]
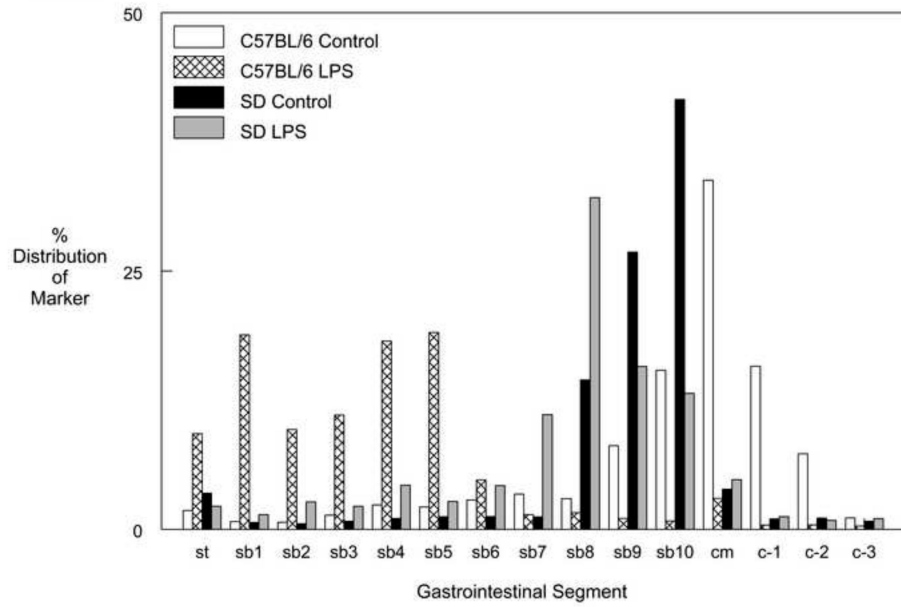
Highlights

➤ Ileus is caused by molecular and cellular inflammatory responses in the gut wall.

➤ Postoperative- and LPS-induced ileus was more severe in mice compared to rats.

➤ Ileus in rat was mediated predominately via a leukocytic pathway.

➤ Mouse ileus evolved via a potent, injury-specific local cytokine response
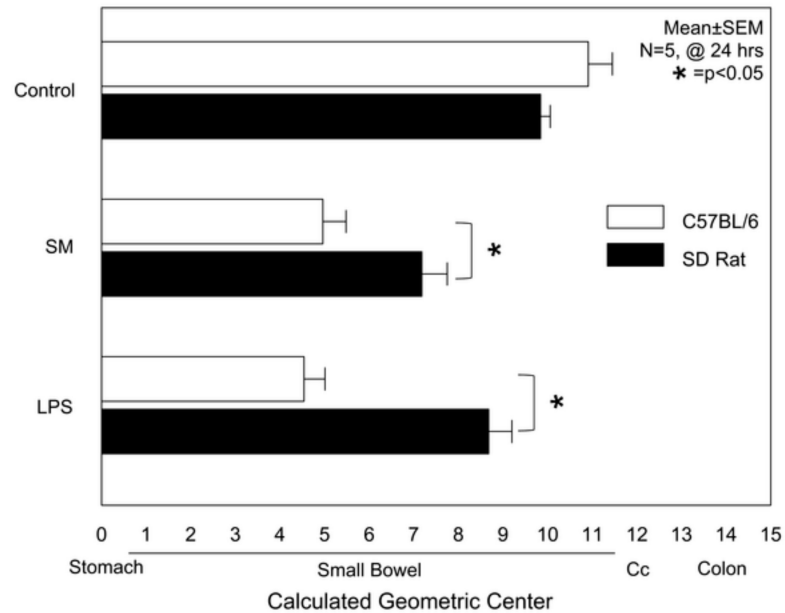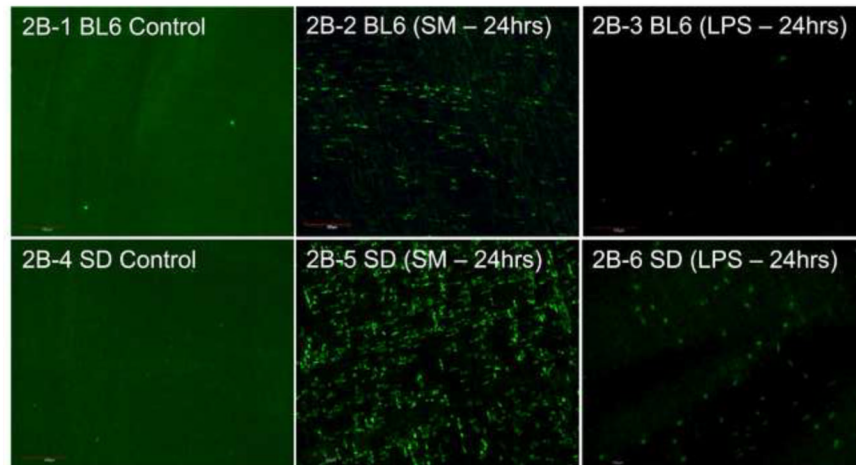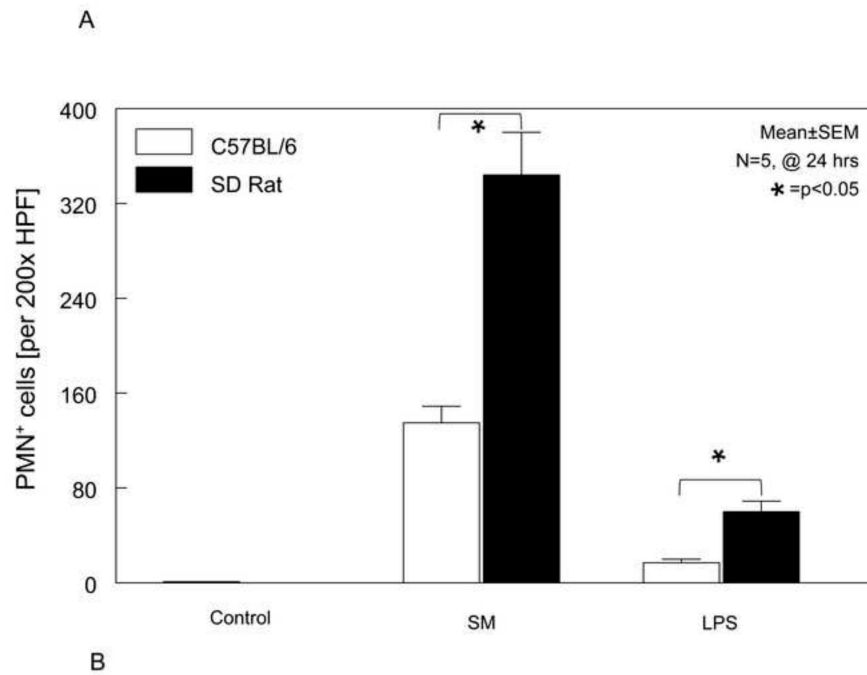
Panel A
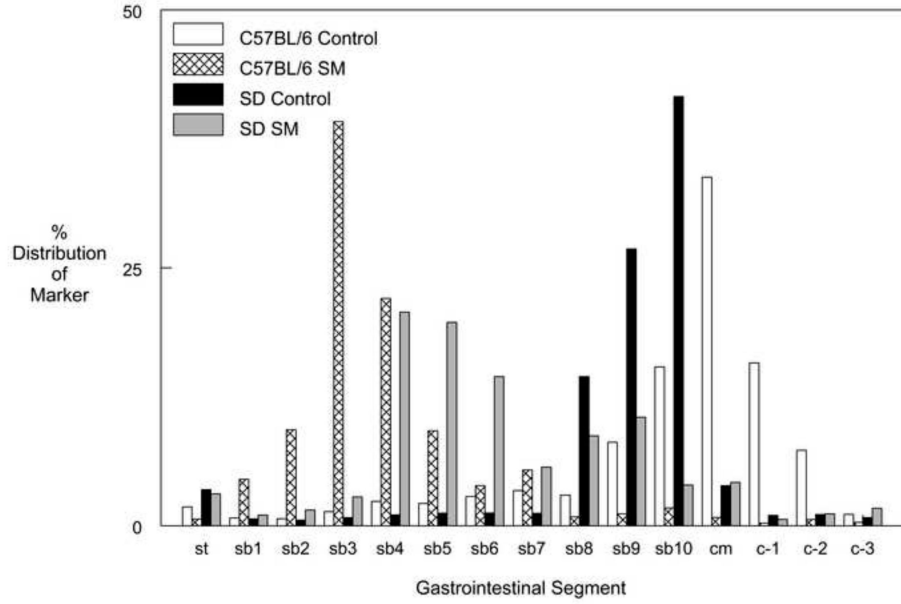
Panel B

Panel C

Figure 1. Surgical Manipulation and Endotoxin Inhibits Gastrointestinal Transit
Panel A: Averaged gastrointestinal transit (GIT) distribution histograms measured in control mice and rats (open and closed bars). Twenty-four hours after surgical manipulation (SM) a delay was observed in GIT of mice (light-grey bars) and rats (dark-grey bars).
Panel B: Averaged GIT distribution histogram data 24 hrs after LPS injection demonstrated a delay in the GIT of mice (light-grey bars) and rats (dark-grey bars) compared to their control groups (mice open and rats closed bars).
Panel C: Calculated geometric centers from the FITC-labeled dextran distribution within the entire rodent digestive tract with normal gastrointestinal passage for both control groups. Postoperative gastrointestinal transit is significantly more delayed in SM mice compared to rats. Twenty-four hours after LPS injection [15mg/kg] rats revealed a significant delay in GIT and again LPS-induced ileus was more severe in mice than rats, similar to surgically induced ileus (mean ± SEM; * p value <0.05, N=5).
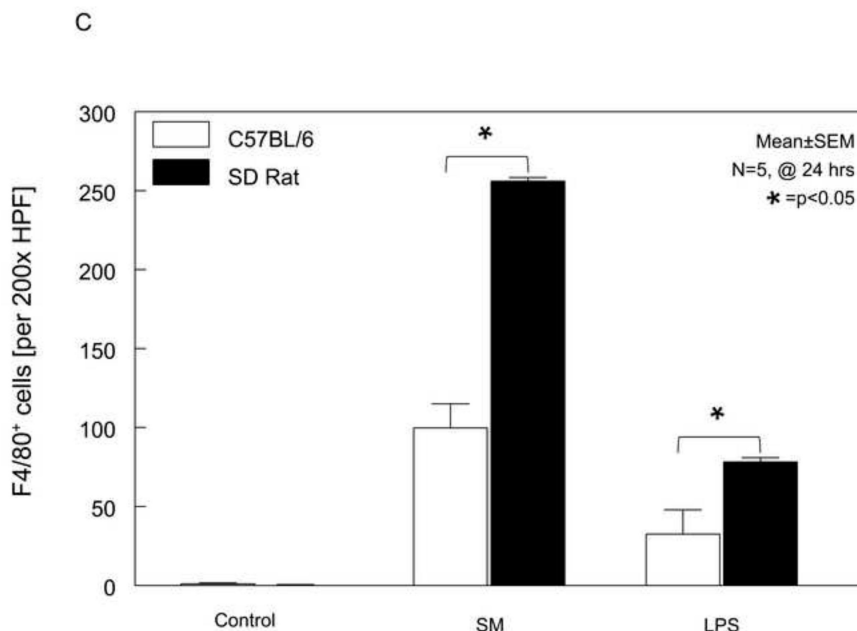
A

B

C

Figure 2. Neutrophil and Monocyte Recruitment into the Small Intestinal Muscularis after Surgical Manipulation and Endotoxin Injection

Panel 2A: Relative to the absence of PMN in both mouse and rat control jejunal muscularis externa, a significant recruitment of MPO+ neutrophils was evident 24 hours after surgical manipulation of the intestine and LPS treatment in both rats and mice. Yet, LPS induced only a modest neutrophil extravasation in both rats and mice compared to surgical manipulation. However, neutrophil transmigration in rats exceeded the cell counts observed in mice for both injury models (data are expressed as mean ± SEM; * p value <0.05, N=5).

Panel 2B: Shown are representative microscopic fields photographed from muscularis externa whole-mounts of all 6 groups stained for the F4/80 monocyte-antigen. Control specimens are lacking infiltrating monocytes (panel 2B-1 and panel 2B-4). After surgical manipulation of the small bowel, an increase in these phagocytes are present in both mouse (panel 2B-2) and even more noticeably in rat (panel 2B-5) after 24 hours. A modest monocyte recruitment was also stimulated in both species 24hrs after LPS injection (mice: panel 2B-3, rats: panel 2B-6) (original magnification 200x).

Panel 2C: The quantification of the muscularis infiltrating F4/80+ monocytes revealed a significant difference between rats and mice for both SM and LPS treatment. Also, the cellular inflammatory response was more intense after surgical manipulation than LPS injection in both species (mean ± SEM; * p value <0.05, N=5).
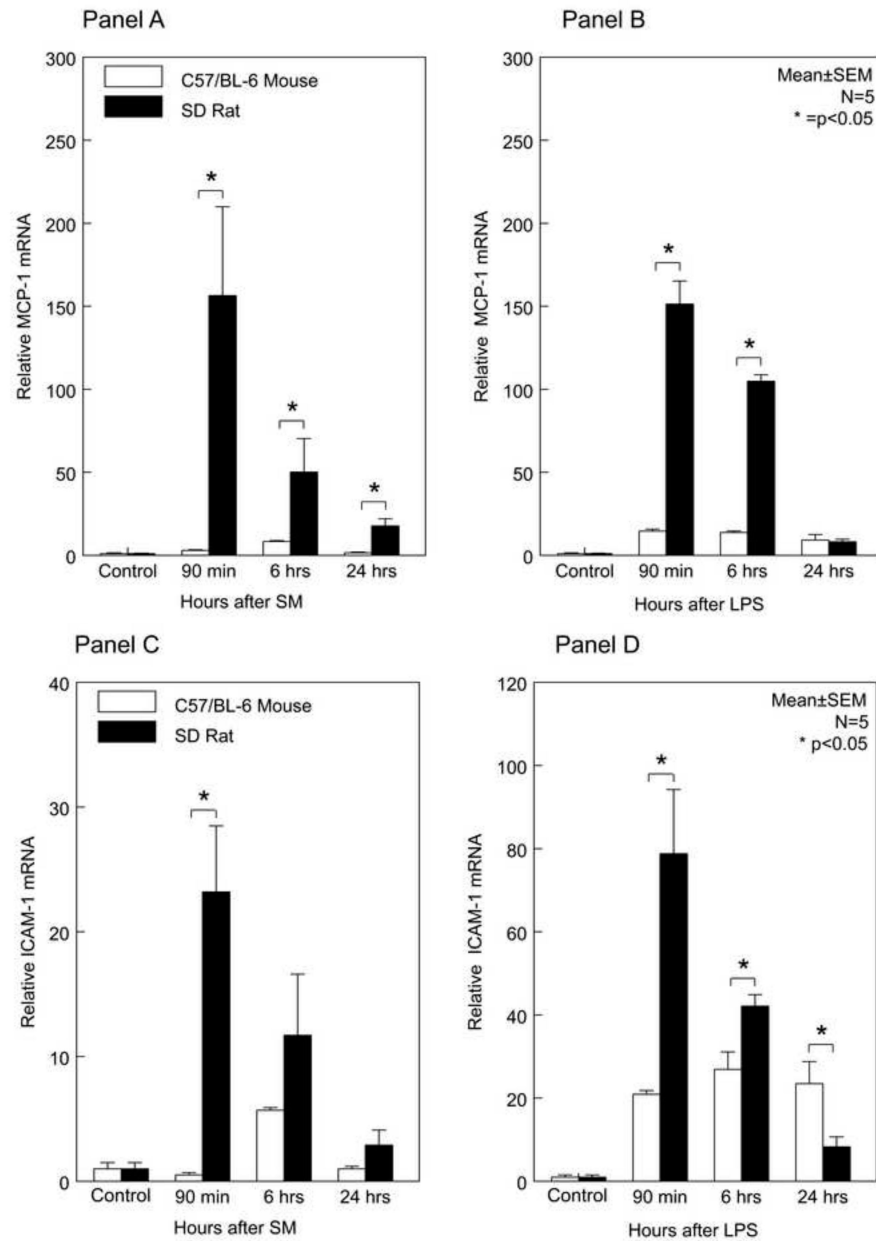
Figure 3. Temporal Induction of Muscularis MCP-1 and ICAM-1 mRNA after Surgical Manipulation and Endotoxin Injection

In rat, SM and LPS-induced MCP-1 mRNA levels were significantly higher over the studied time period compared to the mice with the exception of 24 hours after LPS treatment. Correlating with the levels of MCP-1 was a significantly greater early induction of ICAM-1 mRNA in both SM and LPS models compared to mouse (mean ± SEM; * p value <0.05, N=5).
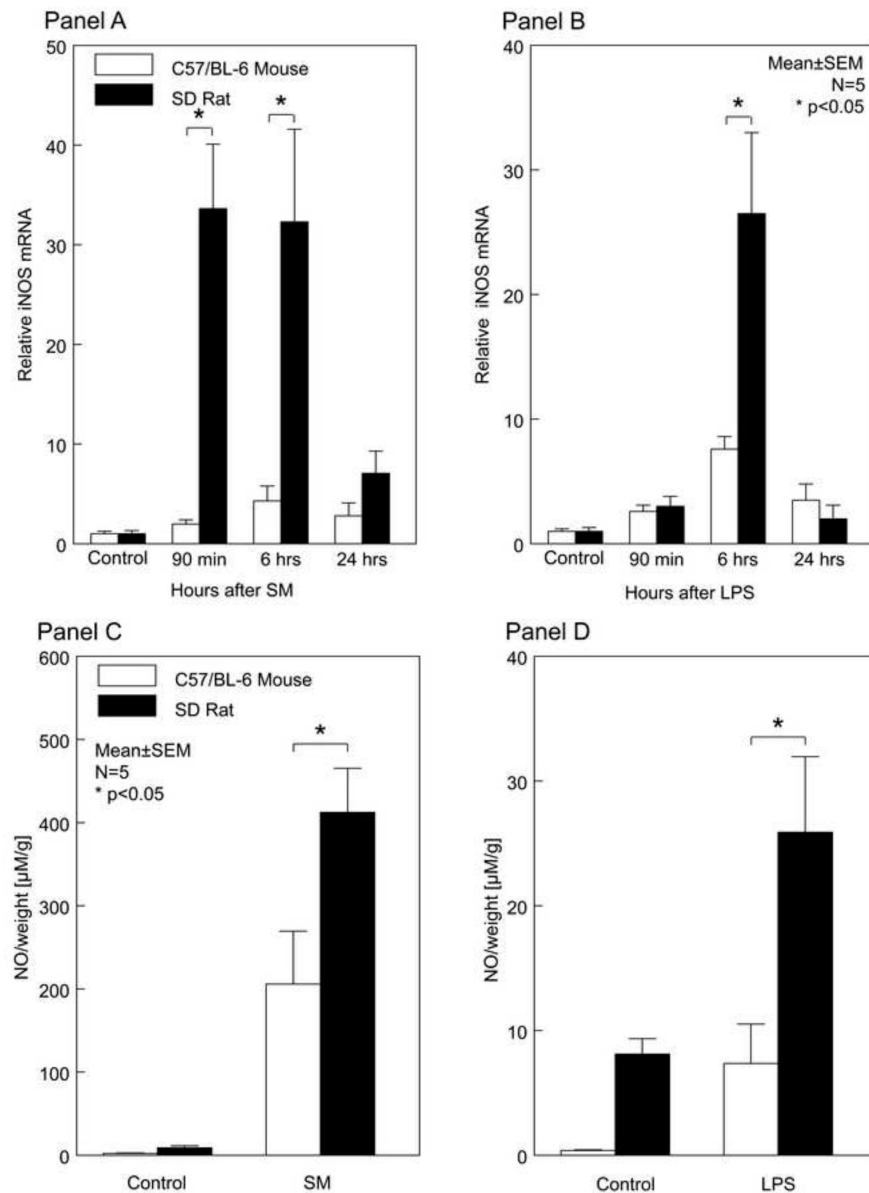
Figure 4. Temporal Induction of iNOS mRNA and muscularis NO Production after Surgical Manipulation and Endotoxin Injection
After surgical manipulation and LPS injection, mouse muscularis iNOS was only moderately expressed over the following postoperative period of 24hrs. In contrast, surgical manipulation rapidly and robustly induced rat muscularis iNOS message (**Panel 4A**) while rat muscularis iNOS mRNA was significantly elevated at 6 hours after LPS injection (**Panel 4B**) (mean ± SEM; * p value <0.05, # p value = 0.07; N=5).
The isolated small intestinal muscularis harvested from untreated control animals released only trace amounts of NO, whereas a significant NO release was measured in the supernatant of organ cultured SM or LPS treated muscularis externa in both mice and rats. Similar to the iNOS molecular expression levels, a significantly higher amount of NO was released after both SM and LPS from the cultured rat muscle compared to NO detected in the supernatant of the incubated mouse smooth muscle tissue (**Panels 4C and 4D**) (mean ± SEM; * p value <0.05, N=5).
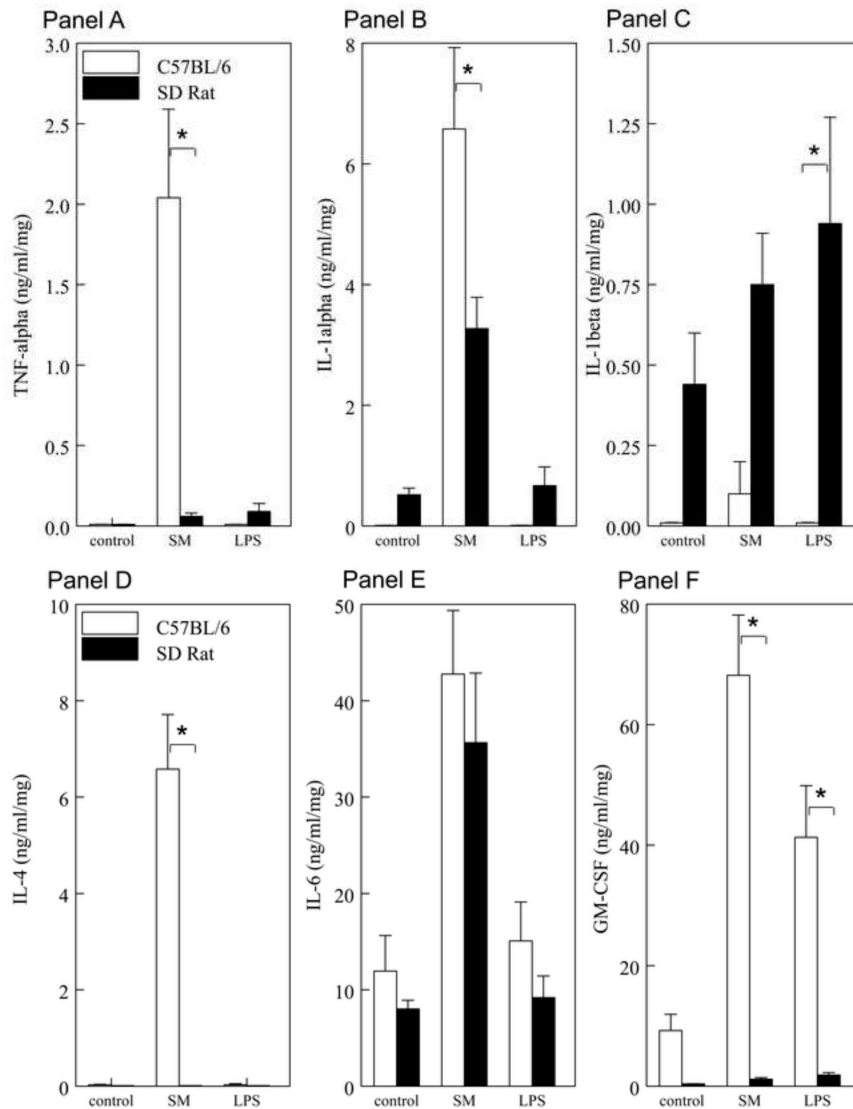
Figure 5. Inflammatory Mediators are differently produced by the cultured muscularis externa after Surgical Manipulation and LPS in Mice and Rats

Luminex multiplex assay quantification and comparison of the liberation of inflammatory proteins into the media of the 24 hr organ cultured muscularis externa of both species after SM and LPS. The inflamed post-surgical mouse muscularis released significantly more TNF-α (Panel A), IL-1-α (Panel B), IL-4 (Panel C) and GM-CSF (Panel F) compared to the rat SM muscularis. LPS initiated the production of significantly more IL-1β in the rat muscularis compared to the mouse, but GM-CSF protein was higher in the mouse compared to the rat after LPS.

Table 1

Nucleotide sequences of oligonucleotide primers C57BL/6 mouse

Target gene . Primer sequences (5′ to 3′)
GAPDH Sense: 5′-TGA AGG TCG GTG TGA ACG GAT TTG GC-3′
Antisense: 3′-CAT GTA GGC CAT GAG GTC CAC CAC-5′
MCP-1 Sense: 5′-CAA CTC TCA CTG AAG CCA GCT CT-3′
Antisense: 3′-CAG GCC CAG AAG CAT GAC A-5′
ICAM-1 Sense: 5′-GTC CGC TGT GCT TTG AGA ACT-3′
Antisense: 3′-CGG AAA CGA ATA CAC GGT GAT-5′
iNOS Sense: 5′-GTG ACG GCA AAC ATG ACT TCA G-3′
Antisense: 3′-GCC ATC GGG CAT CTG GTA-5′

Table 2

Nucleotide sequences of oligonucleotide primers SD rat

Target gene . Primer sequences (5′to 3′)
GAPDH Sense: 5′-ATG GCA CAG TCA AGG CTG AGA-3′
Antisense: 3′-CGC TCC TGG AAG ATG GTG AT-5′
MCP-1 Sense: 5′-CAG CCA GAT GCA GTT AAT GCC-3′
Antisense: 3′-AGC CGA CTC ATT GGG ATC AT-5′
ICAM-1 Sense: 5′-CGT GGC GTC CAT TTA CAC CT-3′
Antisense: 3′-TTA GGG CCT CCT CCT GAG C-5′
iNOS Sense: 5′-GGA GAG ATT TTT CAC GAC ACC C-3′
Antisense: 3′-CCA TGC ATA ATT TGG ACT TGC A-5